

Long-lived connection between southern Siberia and northern Laurentia in the Proterozoic

R. E. Ernst^{1,2*}, M. A. Hamilton³, U. Söderlund⁴, J. A. Hanes⁵, D. P. Gladkochub⁶, A. V. Okrugin⁷, T. Kolotilina⁸, A. S. Mekhonoshin⁸, W. Bleeker⁹, A. N. LeCheminant¹⁰, K. L. Buchan⁹, K. R. Chamberlain¹¹ and A. N. Didenko¹²

Precambrian supercontinents Nuna-Columbia (1.7 to 1.3 billion years ago) and Rodinia (1.1 to 0.7 billion years ago) have been proposed. However, the arrangements of crustal blocks within these supercontinents are poorly known. Huge, dominantly basaltic magmatic outpourings and intrusions, covering up to millions of square kilometres, termed Large Igneous Provinces, typically accompany (super) continent breakup, or attempted breakup and offer an important tool for reconstructing supercontinents. Here we focus on the Large Igneous Province record for Siberia and Laurentia, whose relative position in Nuna-Columbia and Rodinia reconstructions is highly controversial. We present precise geochronology—nine U–Pb and six Ar–Ar ages—on dolerite dykes and sills, along with existing dates from the literature, that constrain the timing of emplacement of Large Igneous Province magmatism in southern Siberia and northern Laurentia between 1,900 and 720 million years ago. We identify four robust age matches between the continents 1,870, 1,750, 1,350 and 720 million years ago, as well as several additional approximate age correlations that indicate southern Siberia and northern Laurentia were probably near neighbours for this 1.2-billion-year interval. Our reconstructions provide a framework for evaluating the shared geological, tectonic and metallogenic histories of these continental blocks.

The Precambrian position of the Siberian craton with respect to Laurentia has been the focus of speculation for nearly four decades. On the basis of mainly geological considerations, Siberia has usually been placed adjacent to northern Laurentia in a wide variety of orientations^{1–3}, or adjacent to western Laurentia⁴. Reconstructions based on palaeomagnetic data have also proved to be controversial because of a paucity of precisely dated (that is, key) palaeopoles from Siberia with which to compare with key poles that are available from Laurentia⁵. Some palaeomagnetists have located Siberia relatively close to the northern Laurentia margin^{6–8}. Others have argued for a large gap between Siberia and northern Laurentia, into which one or more cratons or smaller crustal blocks could be fitted^{9–11}. Still other palaeomagnetists have placed Siberia along the western margin of Laurentia¹², or far to the northeast of Laurentia with one or more cratonic blocks in between^{13,14}. See detailed discussion in Supplementary Section 1.

LIP method for reconstruction

Large Igneous Provinces (LIPs), and especially their associated regional mafic dyke swarms, represent robust tools for rigorous continental reconstruction¹⁵. Here we make use of LIPs in a case study that suggests southern Siberia and northern Laurentia were near neighbours for more than a billion years (from the late Palaeoproterozoic era to the mid Neoproterozoic era).

LIPs are large-volume intraplate magmatic events (>100,000 km³) consisting of volcanic rocks (mainly flood basalts), gabbro/dolerite sill complexes, mafic–ultramafic layered

intrusions, and a plumbing system of dolerite dyke swarms¹⁶. LIPs are typically characterized by a short-duration magmatic pulse or pulses (each less than 1–5 Myr), and, although various origins have been proposed, most models begin with the ascent of deep-seated mantle plumes to the base of Earth's lithosphere. The multi-stage breakup history of Pangea, Earth's most recent supercontinent, demonstrates that LIPs play a pivotal role in continental breakup, typically leaving remnants of flood basalts and their giant feeder dyke swarms (both radiating and linear) on conjugate rifted margins¹⁶. LIPs can now be routinely dated precisely and accurately using the U–Pb method on baddeleyite and zircon^{17–19}.

Multiple precisely dated events provide a magmatic 'barcode' of ages that 'fingerprint' a crustal block^{20,21}. These 'barcodes' can be compared between different crustal blocks (for example, Fig. 1), to recognize original 'nearest neighbours' that shared magmatic components of the same LIP(s). In addition, the geometry of radiating dyke swarms can define the relative orientation of blocks, while primary palaeomagnetic information (based mainly on LIP units) can constrain orientation, latitude, and relative longitude.

Magmatic links of southern Siberia and northern Laurentia

The nine U–Pb baddeleyite ages and six Ar–Ar amphibole and biotite ages (on LIP units) that are presented in this paper (Supplementary Information), along with earlier published geochronology, indicate a number of LIP age matches that support

¹Department of Earth Sciences, Carleton University, Ottawa, Ontario K1S 5B6, Canada. ²Faculty of Geology and Geography, Tomsk State University, Tomsk 634050, Russia. ³Jack Satterly Geochronology Laboratory, University of Toronto, Toronto, Ontario M5S 3B1, Canada. ⁴Department of Earth and Ecosystem Sciences, Lund University, 223 62 Lund, Sweden. ⁵Department of Geological Sciences and Geological Engineering, Queen's University, Kingston, Ontario K7L 3N6, Canada. ⁶Institute of the Earth's Crust, Siberian Branch of the RAS, Irkutsk 664033, Russia. ⁷Diamond and Precious Metal Geology Institute, Yakutsk 677000, Russia. ⁸Institute of Geochemistry, Irkutsk 664033, Russia. ⁹Geological Survey of Canada, Ottawa, Ontario K1S 0E8, Canada.

¹⁰Geological Survey of Canada (retired), 5592 Van Vliet Road, Manotick, Ontario K4M 1J4, Canada. ¹¹Department of Geology and Geophysics, University of Wyoming, Laramie, Wyoming 82071, USA. ¹²Kosygin Institute of Tectonics and Geophysics, Khabarovsk 680063, Russia.

*e-mail: Richard.Ernst@ErnstGeosciences.com

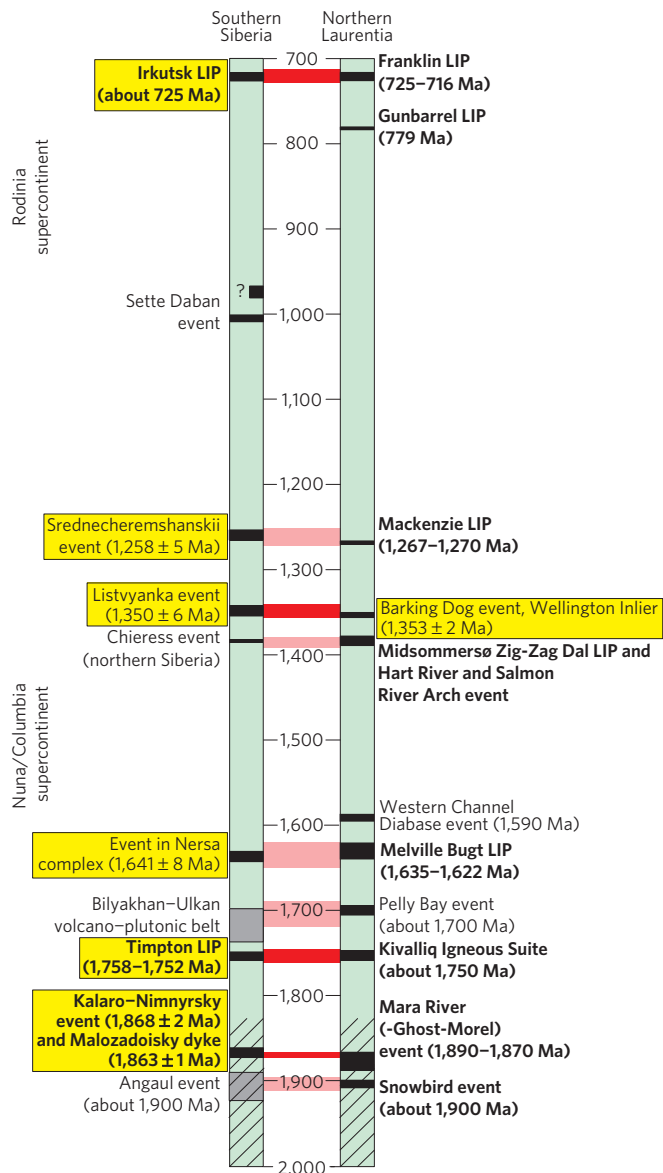


Figure 1 | LIP event barcodes for southern Siberia and northern Laurentia (apart from the Chieress event, which is from northern Siberia). Largest events (see Fig. 2) are in bold text. The red bars identify indistinguishable ages between LIP units of southern Siberia and northern Laurentia. The pink bars indicate approximate age correlations (and the precise age match between the 1,380 Ma event of northern Siberia and Greenland). U–Pb dates presented herein (see details in Supplementary Information) are highlighted in yellow. Referencing for geochronology of other units is presented in the text.

a close fit of southern Siberia against northern Laurentia from the late Palaeoproterozoic to the mid Neoproterozoic.

A small separation between the southern Siberia and northern Laurentia blocks is necessary to accommodate a restored North Slope subterrane of Alaska (Fig. 2), recently shown to preserve a record of magmatism 720 Myr ago (720 Ma)²². In addition, there is debate on whether Pearya of northern Ellesmere Island²³ and other small terranes, at present in northern Russia, were attached to northern Laurentia at this time¹¹.

Key LIP correlations between Laurentia–Siberia. 725–715 Ma Franklin LIP versus Irkutsk LIP. The 725–715 Ma Franklin LIP (Fig. 2a) extends over an area of >3 Mkm² and consists of units

such as the Coronation gabbro sills (Co), Minto Inlier basalts and sills (MI) and Mount Harper volcanics (MH) in northern Canada and equivalent units in reconstructed northwestern Greenland^{24–29}. Most prominently, the radiating Franklin dolerite dyke swarm (F) converges towards the northern margin of Laurentia (north of Banks Island), marking a probable mantle plume centre (indicated by a star) and potential Neoproterozoic breakup margin. Franklin-age Kikiktat flood basalts (Ki) have recently been recognized in the North Slope subterrane of Alaska which may have originally been located north of Laurentia, between reconstructed Laurentia and Siberia²² (Fig. 2b).

The Irkutsk LIP of southern Siberia consists of Ni–Cu–PGE ore-bearing dunite–peridotite–pyroxenite–gabbro complexes: Dovyren (D) intrusive massif (724 ± 3 Ma, U–Pb baddeleyite, Supplementary Section 3-2.1; 728 ± 3 Ma, U–Pb zircon laser ablation³⁰), and associated volcanic rocks from the Inyaptuk Formation (729 ± 14 Ma; ref. 30), Verkhni (Upper) Kingash (UK) (726 ± 18 Ma, U–Pb, Supplementary Section 3-2.2), and the Tartai (T) intrusion (713 ± 6 Ma, U–Pb SHRIMP³¹). The Sayan (S) and Baikal (B) dykes, with Ar–Ar dates of ~700–800 Ma (ref. 32) are provisionally considered part of this LIP; they converge along the margins of the Irkutsk Promontory, suggesting that they are part of a radiating swarm. The predicted continuation of the radiating pattern between these areas is obscured by younger cover rocks in the interior of the Irkutsk Promontory. The inferred plume centre (indicated by a star) defined by the Franklin radiating swarm can therefore be provisionally overlapped with a plume centre proposed for the converging Sayan and Baikal dykes. Furthermore, the Yenisei uplift (Y) hosts rifts and rift-related magmatism dated as ~730–720 Ma (ref. 33).

1,350 Ma Barking Dog event versus Listvyanka event. An unexpected new age for mafic magmatism in Siberia was revealed by a date of 1,350 ± 6 Ma for a 30-m-wide dolerite dyke of the Listvyanka (L) swarm in the Irkutsk region (Fig. 2e), and this is synchronous with the 1,353 ± 2 Ma Barking Dog (BD) gabbro sill from the Wellington Inlier of Victoria Island, northern Canada (U–Pb baddeleyite ages, Supplementary Sections 3-4.1 and 3-4.2).

1,760–1,750 Ma Kivalliq event versus Timpton LIP. The 1,759–1,752 Ma Timpton LIP of Siberia (Fig. 2j) consists of a giant radiating dolerite dyke swarm with three subswarms: the NW-trending Eastern Anabar (EA) subswarm of the Anabar shield, the SW-trending Chaya (Ch) subswarm of the Lake Baikal area, and the SE-trending Timptano–Algamaisky (TA) subswarm of the Aldan shield³². Precise dates include 1,754 ± 5 and 1,759 ± 4 Ma (U–Pb baddeleyite, Supplementary Sections 3-6.1 and 3-6.2) for two separate dykes of the Timptano–Algamaisky subswarm, and 1,752 ± 3 Ma (U–Pb baddeleyite) for the SW-trending Chaya subswarm in the Baikal region³². In addition, matching Ar–Ar dates of ~1,750 Ma were obtained from three dykes of the SE-trending Timptano–Algamaisky subswarm (Supplementary Section 3-6.3) and from one dyke of the NNW-trending Eastern Anabar subswarm (Supplementary Section 3-6.3).

The widespread Timpton event has a direct age correspondence with the Kivalliq Igneous Suite (~1.75 Ga) of northern Laurentia, which includes the Nueltin (Nu) granite intrusions, gabbro and anorthosite intrusions, basalt, rhyolite and pyroclastic rocks of the Pitz Formation (Wharton Group, middle Dubawnt Super-group) and related mafic dyke swarms, including the McRae (Mc), Hadley Bay (H) and Cleaver (Cl)^{21,34}.

Note that an inferred 1,750 Ma Timpton plume centre (indicated by a star) is well defined by the converging dyke swarms of Siberia, but is distinct from the coeval magmatic centre (indicated by a star) inferred by Peterson³⁴ for the Kivalliq event of northern Laurentia (Fig. 1j). This pattern is in contrast to that observed for other

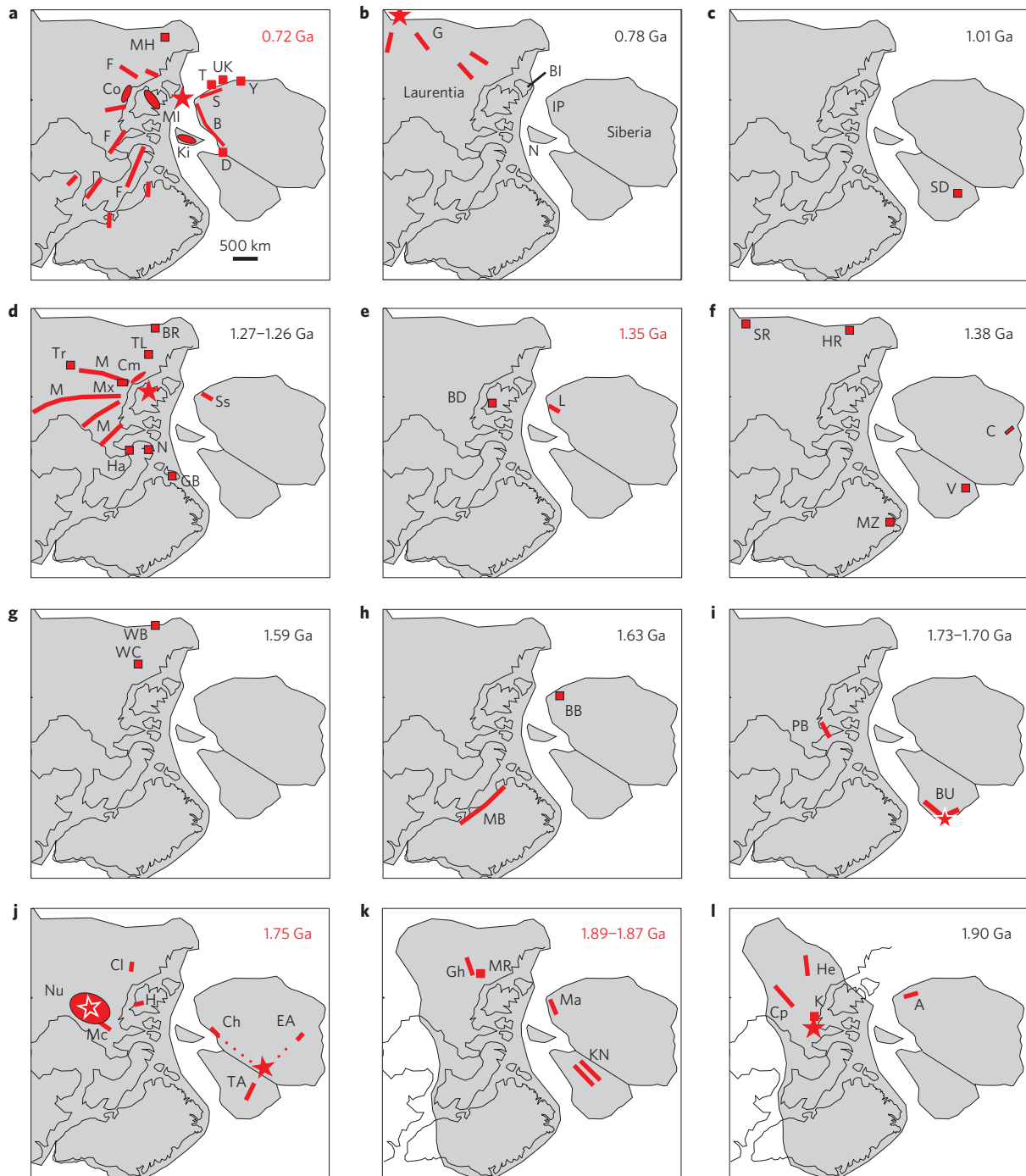


Figure 2 | LIP events of southern Siberia and northern Laurentia. a–l, Units grouped by age. Those with age labels in red font (**a,e,j,k**) represent the most robust correlations. Reconstruction is similar to that in ref. 7, but with extra separation for the North Slope subterrane of Alaska (N) (ref. 22). Details on the reconstruction are provided in Methods. Labels for magmatic units are explained in the text, where the individual panels are discussed. For the two oldest time slices (**k,l**) only the shaded parts of Laurentia were assembled at these times⁴⁶. In **b** BI represents Banks Island and IP represents Irkutsk Promontory.

matching events. For instance, the ~720 Ma magmatism of reconstructed Laurentia (Franklin LIP) and Siberia (Irkutsk LIP) (Fig. 2a) can be linked to a single plume centre. Similarly the ~1,260 Ma dyke in Siberia approximately converges towards the 1,267–1,270 Ma Mackenzie plume centre (see below; Fig. 2d). Typically, a rising plume produces a LIP associated with a single plume centre¹⁶, as in Fig. 2a,d. However, it is also possible for a plume to spread along the base of thick lithosphere and ascend in widely separated lithospheric thinspots^{16,35}. Such a scenario could explain the presence of the two distinct magmatic centres (stars) dated as 1,750 Ma in reconstructed

Siberia and Laurentia (Fig. 2j) or the two apparent nodes of 1,380 Ma magmatism in Laurentia (see below; Fig. 2f).

1,870 Ma Mara River event versus Kalaro–Nimnyrsky event. Ar–Ar dates of ~1.87 Ga on two dykes, including one determination at $1,868 \pm 8$ Ma (Supplementary Section 3-7.3), and a precise U–Pb date of $1,869 \pm 2$ Ma on one dyke (Supplementary Section 3-7.1), were obtained for the Kalaro–Nimnyrsky (KN) swarm (Fig. 2k) of the Aldan shield of Siberia. This >400-km-long swarm is co-linear with the major 150-m-wide Malozadoisky (Ma) dyke in

the Sharazhalgai block, dated at $1,863 \pm 1$ Ma (U–Pb baddeleyite, Supplementary Section 3-7.2), and if linked would yield a combined swarm length of 1,500 km, suggesting that this giant swarm represents a LIP plumbing system. A thin 0.5-m-wide dyke dated at $1,864 \pm 4$ Ma (U–Pb zircon), also in the Sharazhalgai block, may be related³⁶; see Supplementary Fig. 5. Widespread ~ 1.87 – 1.85 Ga silicic intrusive rocks in the region³² could also be related via melting of lower crust resulting from magmatic underplating associated with the Kalaro–Nimnysky LIP (see discussion of silicic provinces associated with LIPs in ref. 16).

The oldest age of this 1,863–1,869 Ma LIP of southern Siberia is indistinguishable in age from that of the Mara River (MR) sheets (dated at 1,870 Ma; U–Pb), and only slightly younger than the $\sim 1,885$ Ma (U–Pb) Ghost (Gh) dolerite dykes^{21,28} and other mafic units in the Slave craton.

Additional possible correlations. 1,270–1,260 Ma Mackenzie LIP versus Srednecheremshanskii event. The 1,267–1,270 Ma Mackenzie LIP of northern Canada (Fig. 2d) consists of remnant flood basalts (Coppermine, Cm, Tweed Lake, TL, Nauyat, N and Hansen, Ha), layered mafic–ultramafic intrusions (for example, Muskox, Mx), dolerite sills (for example, Tremblay, Tr, Goding Bay, GB), Bear River dykes (BR), and most markedly the giant radiating Mackenzie (M) dolerite dyke swarm that extends $>2,000$ km and fans over an angle of $>90^\circ$ across the northern Canadian Shield^{21,24,28,37}; the entire event extends over an area of at least 3 Mkm².

The 200-m-wide Srednecheremshanskii (Ss) mafic–ultramafic dyke in southern Siberia is dated at $1,258 \pm 5$ Ma (U–Pb baddeleyite, Supplementary Section 3-3.1), which is slightly younger than the 1,267–1,270 Ma date for the Mackenzie LIP. In our reconstruction (Fig. 2d) this dated dyke trends towards the well-defined Mackenzie plume centre (indicated by a star). However, further U–Pb dating of subparallel dykes is required to clarify whether the age range of Srednecheremshanskii magmatism overlaps with the precisely dated Mackenzie LIP.

1,380 Ma Midsommersø and Hart River versus Chieress events. There are two distinct nodes of $\sim 1,380$ Ma magmatism in Laurentia (Fig. 2f)²¹. In western Laurentia, these include the 1,380 Ma (U–Pb) Hart River (HR) volcanic rocks and dolerite sills, as well as coeval sills located further south in the Salmon River Arch area of the Belt Basin (SR). A second distinct node of 1,380 Ma activity, located in northeastern Laurentia, is represented by the 1,380 Ma Midsommersø diabase sills and related Zig–Zag Dal flood basalts (MZ) of northeast Greenland³⁸. These events are matched in Siberia by the $1,384 \pm 2$ Ma (U–Pb baddeleyite) Chieress swarm (C) in northern Siberia³⁹, and potentially by a dolerite (V) dated at $1,339 \pm 54$ Ma (Sm–Nd) in the Sette Daban region of the Verkhoyansk belt of southeastern Siberia³².

1,630 Ma Melville Bugt event versus Biryusa Block sill event. The SW side of the Irkutsk Promontory hosts the Biryusa block dolerite sills (BB) (Fig. 2h), which previously yielded multiple emplacement dates of 741 ± 2 Ma (Ar–Ar, plagioclase), 612 ± 6 Ma (Ar–Ar, plagioclase) and 511 ± 5 Ma (U–Pb, zircon)^{32,40}. Another dolerite sill has yielded a much older date of $1,641 \pm 8$ Ma (U–Pb, baddeleyite, Supplementary Section 3-5.1). This Mesoproterozoic age for a sill in the Biryusa block is evidence for a previously unrecognized intraplate event in southern Siberia that can speculatively be linked with the 1,000-km-long 1,635–1,620 Ma Melville Bugt (MB) dolerite swarm of Greenland⁴¹.

1,700 Ma Pelly Bay event versus Bilyakchan–Ulkan event. The EW-trending Pelly Bay (PB) swarm (Fig. 2i) ($\sim 1,700$ Ma; ref. 42) of northern Laurentia trends towards the $\sim 1,700$ – $1,740$ Ma Bilyakchan–Ulkan (BU) anorogenic volcanic–plutonic rift belt,

which extends for more than 750 km along the southeastern side of the Siberian craton and consists of two intervals: a pre-rift stage (1,736–1,727 Ma) and a rift stage proper (1,722–1,705 Ma)^{8,43}. Overall, Bilyakchan–Ulkan magmatism and rifting could be related to a plume centre (indicated by a star), but its relationship with the slightly older 1,750 Ma Tipton plume centre (Fig. 2j) remains to be fully understood.

1,900 Ma Snowbird event versus Angaul event. The ~ 1.90 Ga Snowbird magmatic event of Laurentia (Fig. 2l), which includes the $1,901 \pm 4$ Ma (U–Pb) Hearne (He) and $\sim 1,896$ Ma Chipman (Cp) dykes, and the $\sim 1,900$ Ma Kramanituur (K) and related intrusions²¹, can be approximately matched with the $1,913 \pm 21$ Ma (U–Pb) Angaul (A) dykes of the Irkutsk Promontory of southern Siberia³². Given their significant thickness (20–80 m, and in some cases, up to 200 m), the Angaul dykes probably belong to a major SE-trending swarm which may strike towards the speculative Snowbird plume centre (indicated by a star) in our reconstruction.

Events currently uncorrelated between Laurentia and Siberia. The 780 Ma Gunbarrel LIP (Fig. 2b; Gunbarrel, G, radiating dyke swarm)⁴⁴, and the 1,590 Ma Western Channel Diabase (WC)⁴⁵ and Wernecke Breccia (WB) events of Laurentia (Fig. 2g) are not yet recognized in Siberia. Nor is the 1.01 (–0.98?) Ga Sette Daban dolerite sill event (SD)³ of eastern Siberia (Fig. 2c) recognized in northern Laurentia. However, many magmatic units in southern Siberia and in some parts of northern Laurentia remain undated or poorly dated. U–Pb dating of these units is predicted to identify new LIP barcode matches and expand the distribution of known correlations (Fig. 2) between southern Siberia and northern Laurentia.

Discussion

Nine LIP barcode matches for northern Laurentia and southern Siberia between $\sim 1,900$ and 720 Ma (Fig. 1) suggest that Siberia and Laurentia were close throughout this long interval. The matching magmatism is in closest proximity in a reconstruction with southern Siberia facing northern Laurentia, as shown in Fig. 2. Most significantly we recognize the continuation of the large 725–715 Ma Franklin LIP of northern Laurentia into southern Siberia (Fig. 2a), as well as the presence of 1,350 and 1,750 Ma (Fig. 2e,) intraplate magmatism in both crustal blocks. Older matches at $\sim 1,900$ and 1,885–1,870 Ma (Fig. 2k,l), before the final assembly of Laurentia and Siberia, suggest a similar fit between the Slave–Rae craton of northern Laurentia⁴⁶ and the southernmost blocks of Siberia. The validity of the reconstruction of Fig. 2 is strengthened because it yields a shared plume centre location for the widespread magmatism at ~ 720 Ma (Fig. 2a) with other speculative shared plume centres at other times. It is broadly similar to a palaeomagnetic reconstruction based on non-key pole comparisons for the 1,880 to 1,380 Ma period⁷, and reconstructions based on the recovery in southern Siberia, but not in northern Siberia, of detrital zircons derived from the Grenvillian orogeny of Laurentia³. The first key palaeomagnetic pole match has recently been reported at 1,880 Ma (ref. 6), and permits Laurentia and Siberia to be approximately in our preferred reconstruction (Fig. 2), although other reconstruction options are also allowed (see discussion in Supplementary Section 1).

On the other hand, it should be noted that, whereas the cratons and orogenic belts of northern Laurentia are relatively well characterized, their conclusive counterparts have yet to be identified in southern Siberia, whose terranes are less well understood^{6,9}. Thus, assessing correlations of belts will require further study, particularly in southern Siberia.

The expanded and precisely dated LIP record does not lend support to other proposed reconstructions of Siberia close to the northern Laurentia margin, in which southern Siberia is

rotated (90°–180°) away from northern Laurentia. In particular, the extensive (700 km across) 1,501 Ma Kuonamka LIP⁴⁷ of northern Siberia has no match in northern Laurentia, and furthermore has been linked with coeval magmatism in the formerly attached São Francisco–Congo craton⁴⁸. Also, any orientation of Siberia other than that shown in Fig. 2 reduces the proximity of most matches, and eliminates overlap of the ~720 Ma plume centres that is shown in Fig. 2a. Similarly, mismatches in the precisely dated LIP barcodes of Siberia and western Laurentia are not consistent with proposed reconstructions in which Siberia is located along the western margin of Laurentia. For example, the widespread 780 Ma event of western Laurentia (Fig. 2b) has no known counterpart in Siberia, and the large 1,501 Ma Kuonamka LIP of northern Siberia (mentioned above) has not been identified in western Laurentia. Once again, the 720 Ma plume centre locations (Fig. 2a) would no longer overlap. A location for Siberia adjacent to western Laurentia has been proposed¹² on the basis of non-key palaeomagnetic poles (many of which are poorly dated), although the methodology used has been criticized⁴⁹, and the reconstruction is not consistent with the recent 1,880 Ma key palaeopole comparison⁶. See discussion in Supplementary Section 1.

In our preferred reconstruction (Fig. 2), we propose that the Irkutsk Promontory (IP in Fig. 2b) of southern Siberia was located near Banks Island of northern Laurentia (BI in Fig. 2b) for over a billion years. In this reconstruction, rifting associated with each of the correlated LIP events must not have led to breakup of the combined Siberia–Laurentia craton, except potentially in the case of the youngest matching event, the voluminous and widespread 720 Ma Franklin and Irkutsk LIP magmatism (Fig. 2a). It should be noted that, whereas many LIPs are linked with continental breakup, some prominent LIPs (for example, the 252 Ma Siberian Trap LIP) led only to attempted breakup and the opening of small basins¹⁶.

The combined Siberia–Laurentia craton, with an area of ~25 Mkm², formed an essential, core component of both the Nuna–Columbia and Rodinia supercontinents (Fig. 1). Our reconstruction (Fig. 2) provides a framework for integrating the geology/tectonics of southern Siberia and northern Laurentia over the period 1.9–0.7 Ga. It predicts that all the matched (and at present unmatched) LIP events (in Fig. 2) have a wider distribution across both southern Siberia and northern Laurentia—to be tested by further U–Pb dating of LIP units, particularly in southern Siberia, where precise dating remains limited. Furthermore, the many new events that we have recognized in Siberia based on our new U–Pb and Ar–Ar dating now become important palaeomagnetic targets. Given the large scale of these shared LIP events, it is likely that many Proterozoic ore deposits (for example, Ni–Cu–PGE and hydrothermal types) scattered across northern Laurentia and southern Siberia are directly, or indirectly, associated with magmatism, heat and fluids from the LIP events⁵⁰. In Fig. 2, the ~720 Ma Ni–Cu–PGE bearing intrusions³¹ of the Irkutsk region are juxtaposed opposite 720 Ma Franklin units in northern Laurentia, highlighting the economic prospectivity of the Franklin LIP.

Methods

Methods and any associated references are available in the [online version of the paper](#).

Received 29 October 2015; accepted 17 March 2016; published online 11 April 2016

References

- Hoffman, P. F. Did the breakout of Laurentia turn Gondwanaland inside-out? *Science* **252**, 1409–1412 (1991).
- Condie, K. C. & Rosen, O. M. Laurentia–Siberia connection revisited. *Geology* **22**, 168–170 (1994).
- Rainbird, R. H. *et al.* U–Pb geochronology of Riphean sandstone and gabbro from southeastern Siberia and its bearing on the Laurentia–Siberia connection. *Earth Planet. Sci. Lett.* **164**, 409–420 (1998).
- Sears, J. W. & Price, R. A. Tightening the Siberian connection to western Laurentia. *Geol. Soc. Am. Bull.* **115**, 943–953 (2003).
- Buchan, K. L. Reprint of ‘Key paleomagnetic poles and their use in Proterozoic continent and supercontinent reconstructions: A review’. *Precamb. Res.* **244**, 5–22 (2014).
- Buchan, K. L., Mitchell, R. N., Bleeker, W., Hamilton, M. A. & LeCheminant, A. N. Paleomagnetism of ca. 2.13–2.11 Ga Indin and ca. 1.885 Ga Ghost dyke swarms of the Slave craton: implications for the Slave craton APW path and relative drift of Slave, Superior and Siberian cratons in the Paleoproterozoic. *Precamb. Res.* **275**, 151–175 (2016).
- Evans, D. A. D. & Mitchell, R. N. Assembly and breakup of the core of Paleoproterozoic–Mesoproterozoic supercontinent Nuna. *Geology* **39**, 443–446 (2011).
- Didenko, A. N., Vodovozov, V. Y., Peskov, A. Y., Guryanov, V. A. & Kosynkin, A. V. Paleomagnetism of the Ulkan brassif (SE Siberian platform) and the apparent polar wander path for Siberia in late Paleoproterozoic–early Mesoproterozoic times. *Precamb. Res.* **259**, 58–77 (2015).
- Pisarevsky, S. A., Natapov, L. M., Donskaya, T. V., Gladkochub, D. P. & Vernikovskiy, V. A. Proterozoic Siberia: a promontory of Rodinia. *Precamb. Res.* **160**, 66–76 (2008).
- Pisarevsky, S. A., Elming, S.-Å., Pesonen, L. J. & Li, Z.-X. Mesoproterozoic paleogeography: supercontinent and beyond. *Precamb. Res.* **244**, 207–225 (2014).
- Li, Z.-X. *et al.* Assembly, configuration, and break-up history of Rodinia: a synthesis. *Precamb. Res.* **160**, 179–210 (2008).
- Piper, J. D. A. The Neoproterozoic supercontinent Palaeopangaea. *Gondwana Res.* **12**, 202–227 (2007).
- Smethurst, N. A., Khramov, A. N. & Torsvik, T. H. The Neoproterozoic and Palaeozoic palaeomagnetic data from the Siberian platform: from Rodinia to Pangea. *Earth Sci. Rev.* **43**, 1–24 (1998).
- Evans, D. A. D. in *Ancient Orogens and Modern Analogues* Vol. 327 (eds Murphy, J. B., Keppie, J. D. & Hynes, A.) 371–405 (Geological Society of London Special Publication, 2009).
- Ernst, R. E., Bleeker, W., Söderlund, U. & Kerr, A. C. Large Igneous Provinces and supercontinents: toward completing the plate tectonic revolution. *Lithos* **174**, 1–14 (2013).
- Ernst, R. E. *Large Igneous Provinces* (Cambridge Univ. Press, 2014).
- Heaman, L. M. & LeCheminant, A. N. Paragenesis and U–Pb systematics of baddeleyite (ZrO₂). *Chem. Geol.* **110**, 95–126 (1993).
- Chamberlain, K. R. *et al.* In situ U–Pb SIMS (IN-SIMS) micro-baddeleyite dating of mafic rocks: method with examples. *Precamb. Res.* **183**, 379–387 (2010).
- Söderlund, U. *et al.* Reply to Comment on ‘U–Pb baddeleyite ages and geochemistry of dolerite dykes in the Bas–Draâ Inlier of the Anti-Atlas of Morocco: newly identified 1380 Ma event in the West African Craton’ by André Michard and Dominique Gasquet. *Lithos* **174**, 101–108 (2013).
- Bleeker, W. & Ernst, R. in *Dyke Swarms – Time Markers of Crustal Evolution* (eds Hanski, E., Mertanen, S., Rämö, T. & Vuollo, J.) 3–26 (Taylor and Francis/Balkema, 2006).
- Ernst, R. E. & Bleeker, W. Large igneous provinces (LIPs), giant dyke swarms, and mantle plumes: significance for breakup events within Canada and adjacent regions from 2.5 Ga to the present. *Can. J. Earth Sci.* **47**, 695–739 (2010).
- Cox, G. M. *et al.* Kikiktat volcanics of Arctic Alaska—Melting of harzburgitic mantle associated with the Franklin Large Igneous Province. *Lithosphere* **7**, 275–295 (2015).
- Hadlari, T., Davis, W. J. & Dewing, K. A pericratonic model for the Pearya terrane as an extension of the Franklinian margin of Laurentia, Canadian Arctic. *Geol. Soc. Am. Bull.* **126**, 182–200 (2013).
- Fahrig, W. F. in *Mafic Dyke Swarms* Vol. 34 (eds Hall, H. C. & Fahrig, W. F.) 331–348 (Geological Association of Canada Special Paper, 1987).
- Heaman, L. M., LeCheminant, A. N. & Rainbird, R. H. Nature and timing of Franklin igneous events, Canada: implications for a Late Proterozoic mantle plume and the break-up of Laurentia. *Earth Planet. Sci. Lett.* **109**, 117–131 (1992).
- Densyzy, S. W., Halls, H. C., Davis, D. W. & Evans, D. A. D. Paleomagnetism and U–Pb geochronology of Franklin dykes in High Arctic Canada and Greenland: a revised age and paleomagnetic pole constraining block rotations in the Nares Strait region. *Can. J. Earth Sci.* **46**, 689–705 (2009).
- Macdonald, F. A. *et al.* Calibrating the cryogenian. *Science* **327**, 1241–1243 (2010).
- Buchan, K. L. *et al.* Proterozoic Magmatic Events of the Slave Craton, Wopmay Orogen and Environs (Geological Survey of Canada, Open File 5985, Natural Resources Canada, 2010).

29. Buchan, K. L. & Ernst, R. E. *Diabase Dyke Swarms of Nunavut, Northwest Territories, and Yukon, Canada* (Geological Survey of Canada, Open File 7464, Natural Resources Canada, 2013).
30. Ariskin, A. A. *et al.* Geochronology of the Dovryen intrusive complex, Northwestern Baikal area, Russia, in the Neoproterozoic. *Geochem. Int.* **51**, 859–875 (2013).
31. Polyakov, G. V. *et al.* Ultramafic–mafic igneous complexes of the Precambrian East Siberian metallogenic province (southern framing of the Siberian craton): age, composition, origin, and ore potential. *Russ. Geol. Geophys.* **54**, 1319–1331 (2013).
32. Gladkochub, D. P. *et al.* Proterozoic mafic magmatism in Siberian craton: an overview and implications for paleocontinental reconstruction. *Precambr. Res.* **183**, 660–668 (2010).
33. Nozhkin, A. D., Kachevskii, L. K. & Dmitrieva, N. V. The Late Neoproterozoic rift-related metarhyolite–basalt association of the Glushikha trough (Yenisei Ridge): petrogeochemical composition, age, and formation conditions. *Russ. Geol. Geophys.* **54**, 44–54 (2013).
34. Peterson, T. D., Scott, J. M. J., LeCheminant, A. N., Jefferson, C. W. & Pehrsson, S. J. The Kivalliq Igneous Suite: anorogenic bimodal magmatism at 1.75 Ga in the western Churchill Province, Canada. *Precambr. Res.* **262**, 101–119 (2015).
35. Bright, R. M., Amato, J. M., Denyszyn, S. W. & Ernst, R. E. U–Pb geochronology of 1.1 Ga diabase in the southwestern United States: testing models for the origin of a post-Grenville Large Igneous Province. *Lithosphere* **6**, 135–156 (2014).
36. Gladkochub, D. P. *et al.* The first evidence of Paleoproterozoic late-collision basite magmatism in the near-Sayan salient of the Siberian craton basement. *Dokl. Earth Sci.* **450**, 583–586 (2013).
37. Baragar, W. R. A., Ernst, R. E., Hulbert, L. & Peterson, T. Longitudinal petrochemical variation in the Mackenzie dyke swarm, northwestern Canadian Shield. *J. Petrol.* **37**, 317–359 (1996).
38. Upton, B. G. J. *et al.* The Mesoproterozoic Zig–Zag Dal basalts and associated intrusions of eastern North Greenland: mantle plume–lithosphere interaction. *Contrib. Mineral. Petrol.* **149**, 40–56 (2005).
39. Ernst, R. E., Buchan, K. L., Hamilton, M. A., Okrugin, A. V. & Tomshin, M. D. Integrated paleomagnetism and U–Pb geochronology of mafic dikes of the eastern Anabar Shield region, Siberia: implications for Mesoproterozoic paleolatitude of Siberia and comparison with Laurentia. *J. Geol.* **108**, 381–401 (2000).
40. Metelkin, D. V. *et al.* Paleomagnetic directions from Nersa intrusions of the Biryusa terrane, Siberian craton, as a reflection of tectonic events in the Neoproterozoic. *Russ. Geol. Geophys.* **46**, 395–410 (2005).
41. Halls, H. C., Hamilton, M. A. & Denyszyn, S. W. in *Keys for Geodynamic Interpretation* (ed. Srivasatava, R. K.) 509–535 (Springer, 2011).
42. Bleeker, W. & Ernst, R. E. in *39th Annual Yellowknife Geoscience Forum Abstracts YKGSF Abstracts Vol. 2011* (eds Fischer, B. J. & Watson, D. M.) 22–23 (Northwest Territories Geoscience Office, 2011).
43. Larin, A. M. Ulkan–Dzhugdzhur Ore-Bearing Anorthosite–Rapakivi Granite–Peralkaline Granite Association, Siberian Craton: age, tectonic setting, sources, and metallogeny. *Geol. Ore Deposits* **56**, 257–280 (2014).
44. Sandeman, H. A., Ootes, L., Cousens, B. & Killian, T. Petrogenesis of Gunbarrel magmatic rocks: homogeneous continental tholeiites associated with extension and rifting of Neoproterozoic Laurentia. *Precambr. Res.* **252**, 166–179 (2014).
45. Hamilton, M. A. & Buchan, K. L. U–Pb geochronology of the Western Channel diabase, northwestern Laurentia: implications for a large 1.59 Ga magmatic province, Laurentia’s APWP and paleocontinental reconstructions of Laurentia, Baltica and Gawler craton of southern Australia. *Precambr. Res.* **183**, 463–473 (2010).
46. Corrigan, D., Pehrsson, S., Wodicka, N. & De Kemp, E. in *Ancient Orogens and Modern Analogues* Vol. 327 (eds Murphy, J. B., Keppie, J. D. & Hynes, A. J.) 457–479 (Geological Society of London Special Publication, 2009).
47. Ernst, R. E. *et al.* The 1501 Ma Kuonamka Large Igneous Province of northern Siberia: U–Pb geochronology, geochemistry, and links with coeval magmatism on other crustal blocks. *Russ. Geol. Geophys.* **57**, 657–675 (2016).
48. Cederberg, J., Söderlund, U., Oliveira, E. P., Ernst, R. E. & Pisarevsky, S. A. U–Pb Baddeleyite Dating of the Proterozoic Pará de Minas Dyke Swarm in the São Francisco Craton (Brazil) – Implications for Tectonic Correlation with the Siberian, Congo and the North China Cratons. *GFF* (in the press, 2016).
49. Li, Z. X. *et al.* How not to build a supercontinent: a reply to J. D. A. Piper. *Precambr. Res.* **174**, 208–214 (2009).
50. Ernst, R. E. & Jowitt, S. M. Large Igneous Provinces (LIPs) and metallogeny. *Soc. Econ. Geol. Spec. Publ.* **17**, 17–51 (2013).

Acknowledgements

This is publication number 53 of the Large Igneous Provinces—Supercontinent Reconstruction—Resource Exploration Project funded by an industry consortium and Canadian grant NSERC CRDPJ 419503-11 (www.supercontinent.org; www.camiro.org/exploration/ongoing-projects CAMIRO Project 08E03).

Author contributions

R.E.E. led and coordinated the research and manuscript preparation. M.A.H. and U.S. produced key ID-TIMS U–Pb ages and their interpretation. J.A.H. produced key Ar–Ar ages and their interpretation. K.R.C. assisted in the interpretation of the geochronology results. A.V.O., T.K., A.S.M. and A.N.L. provided key samples for U–Pb dating and assisted in the interpretation of their results. D.P.G. and A.N.D. assisted in the interpretation of the Russian data and its geological context. W.B. provided insight into the LIP correlations and their limitations. K.L.B. provided the background palaeomagnetic context. M.A.H., K.L.B. and A.N.L. were also heavily involved in aspects of preparation, revision and/or finalizing of the overall manuscript.

Additional information

Supplementary information is available in the [online version of the paper](#). Reprints and permissions information is available online at www.nature.com/reprints. Correspondence and requests for materials should be addressed to R.E.E.

Competing financial interests

The authors declare no competing financial interests.

Methods

Producing the reconstruction in Fig. 2. The reconstruction in Fig. 2 was generated as follows. Laurentia is shown straddling the palaeoequator at 1,270 Ma based on the palaeomagnetic pole for the Mackenzie dyke swarm. Siberia has been rotated with respect to Laurentia about an Euler pole at 76.5° N, 100° E (angle $+153^\circ$). Greenland has been rotated with respect to North America about an Euler pole at 65.7° N, 241.5° E (angle -13.8°) following ref. 51. The Aldan block of Siberia has been rotated with respect to the Anabar–Angara block about an Euler pole at 60° N, 115° E (angle $+25^\circ$) following ref. 14 to account for proposed relative rotation in the Devonian period⁵². For the two oldest time slices (Fig. 2k and l) only the shaded parts of Laurentia were assembled at these times^{14,46,53}. The shaded area in Fig. 2k encompasses Slave, Wopmay and Churchill provinces, with the Churchill Province assumed to extend across Greenland under the ice cap. The shaded area in Fig. 2l is the same as in Fig. 2k with the further exclusion of the Wopmay orogen.

Geochronology. New U–Pb and Ar–Ar data were produced for this paper according to the following methodologies:

U–Pb ID-TIMS dating of baddeleyite and zircon. New U–Pb age determinations in this paper (see Supplementary Data) were produced using conventional isotope dilution thermal ionization mass spectrometry (ID-TIMS) methods. The laboratories at Lund University and University of Toronto were used and their methodologies are presented.

For the processing at Lund University, small samples (0.2–0.3 kg) of coarse to medium grained dolerite were processed using the procedure of Söderlund and Johansson⁵⁴ to separate baddeleyite grains of size typically 40–80 μ m in longest dimension. The ID-TIMS isotopic data were collected using a Finnigan Triton thermal ionization mass spectrometer at the Museum of Natural History in Stockholm. Pb and U isotopic data were collected over the temperature ranges 1,180–1,230 °C and 1,260–1,350 °C, respectively. The U decay constants used are from Jaffey and colleagues⁵⁵. A mass discrimination correction of 0.1% per atomic mass unit was applied for Pb, whereas U was internally corrected by measuring masses of ²³³U and ²³⁶U for each scan (ratio close to unity in the spike solution). Laboratory Pb blanks decreased over the analytical period of this study, with the assigned blank falling in the 2.0–0.5 pg range, whereas U was assigned an amount one-tenth that of the Pb blank. Data reduction was performed using an Excel-based program (written by Per-Olof Persson, Museum of Natural History, Stockholm) applying the same algorithms as those in the MS-DOS version (Pb-dat) written by Ludwig⁵⁶. Data regressions and Concordia plots were made using the Isoplot Excel Add-in of Ludwig⁵⁷. Reported age errors are given at the $\pm 95\%$ confidence 2σ level and calculated by propagating the uncertainties in measured isotopic ratios, uncertainty in the fractionation correction (for Pb only), and uncertainties in the isotopic composition of the laboratory blank. Full details are given in Nilsson and colleagues⁵⁸.

Sample processing at the University of Toronto was carried out in the Jack Satterly Geochronology Laboratory, beginning with conventional jaw crushing and disk milling techniques. The initial concentration of zircon was determined by multiple passes on a Wilfley table, followed by magnetic separations using a Frantz isodynamic separator and density separations using methylene iodide. For baddeleyite recovery, samples typically ranging in size from 0.15 to 0.30 kg were processed with a Wilfley table only, using the methods outlined in Hamilton and Buchan⁴⁵. Final sample selection was made by hand-picking under a binocular microscope, choosing the freshest, least-cracked, core- and inclusion-free grains of zircon, and the highest-quality baddeleyite crystals (typically striated blades or blade fragments) as free as possible of zircon frostings or overgrowths. Pretreatment of zircon included either air- or chemical abrasion, as indicated. Zircon and baddeleyite fractions were washed and loaded into Teflon bombs with concentrated HF along with a mixed ²⁰⁵Pb–²³⁵U isotopic tracer solution⁵⁹. The isotopic compositions of Pb and U were measured using a single Daly collector with a pulse counting detector on a solid source VG354 mass spectrometer. A detector mass discrimination of 0.053% per atomic mass unit (AMU) and a dead time of 22.8 ns were employed for Daly detector measurements. A thermal source mass discrimination correction of 0.1% per atomic mass unit was applied for both Pb and U. The assigned laboratory blank for U was 0.2 pg, whereas that for Pb is routinely measured below 1 pg. Error estimates were calculated by propagating known sources of analytical uncertainty for each analysis, including within-run ratio variability, uncertainty in the fractionation correction, and uncertainties in the isotopic composition of the laboratory blank. Initial corrections were made using an in-house data reduction program. Uncertainties for the ID-TIMS data are given at the 95% (2σ) confidence level. Decay constants used in age calculations are those of Jaffey and colleagues⁵⁵. Graphical data presentation and quoted ages were generated using the Microsoft Excel Add-in Isoplot/Ex v. 3.00 of Ludwig⁵⁷. Full details are provided in Hamilton and Buchan⁴⁵.

⁴⁰Ar/³⁹Ar-isotope analyses. ⁴⁰Ar/³⁹Ar analyses were performed at Queen's University, Kingston, on aliquots of amphibole and biotite obtained by crushing chips of the dyke sample with a steel mortar and pestle, and then hand-picking individual grains using tweezers under a binocular microscope. The dyke samples contained very little amphibole and biotite, and thus many hours, and in some cases days, were required to obtain sufficient grains from a dyke. Each mineral separate, consisting of anywhere from as few as ~20 to as many as ~200 mineral grains, was wrapped separately in Al foil, and all of the foil packets were stacked vertically in an Al canister (11.5 cm long \times 2.0 cm diameter), interspersed with packets of the irradiation standard Hb3gr hornblende [K/Ar age = $1,072 \pm 11$ Myr (1σ)]^{60,61}. The samples were irradiated for 42 h at the McMaster Nuclear Reactor.

For the ⁴⁰Ar/³⁹Ar analyses, aliquots of grains were step-heated using an 8 W Lexel 3500 continuous argon-ion laser. The laser beam was defocused to heat the entire sample and only refocused in the last step to fuse the sample. Samples were heated for 3 min at each step, and stepwise-degassed using laser-power increments from approximately 0.5 to 7 W. The released gas was purified with SAES getters, and analysed using a MAP 216 noble-gas mass spectrometer, with a Baur–Signer ion source and an electron multiplier. All ages were calculated using the decay constant as recommended by Steiger and Jäger⁶²: $\lambda_e = 0.581 \times 10^{-10} \text{ yr}^{-1}$, $\lambda\beta = 4.962 \times 10^{-10} \text{ yr}^{-1}$ and $40 \text{ K} = 1.167 \times 10^{-2} \text{ atm}\%$. All isotope analyses were corrected for system blanks (typical blank values were 40×10^{-13} and $75 \times 10^{-13} \text{ cm}^3 \text{ STP}$ for the ⁴⁰Ar peak) run before analysing the gas, atmospheric contamination, and neutron-induced interferences (including the radioactive decay of the ³⁷Ar and ³⁹Ar isotopes). Peaks from ³⁶Ar to ⁴⁰Ar were scanned eight times each, extrapolated back to the inlet time, and standard deviations at 1σ of the peaks were calculated by error-weighted linear regression. Age uncertainties (plateau/plateau segments and integrated ages) were calculated using the standard error-propagation formula applied to the Ar/Ar age equation, which also includes the error of the J-value. A plateau is defined here as three or more contiguous gas fractions on an age-spectrum plot which have apparent ages indistinguishable at the 2σ level and which comprise over 50% of the ³⁹Ar released from the sample. The term 'plateau-segment' is used in those cases where the criteria are not strictly met.

References

- Roest, W. R. & Srivastava, S. P. Sea-floor spreading in the Labrador Sea: a new reconstruction. *Geology* **17**, 1000–1003 (1989).
- Pavlov, V. E., Bachtadse, V. & Mikhailov, V. New Middle Cambrian and Middle Ordovician palaeomagnetic data from Siberia: Llandelian magnetostratigraphy and relative rotation between the Aldan and Anabar–Angara blocks. *Earth Planet. Sci. Lett.* **276**, 229–242 (2008).
- Eglinton, B. M. *et al.* A domain-based digital summary of the evolution of the Palaeoproterozoic of North America and Greenland and associated unconformity-related uranium mineralization. *Precamb. Res.* **232**, 4–26 (2013).
- Söderlund, U. & Johansson, L. A simple way to extract baddeleyite (ZrO₂). *Geochim. Geophys. Geosyst.* **3**, <http://dx.doi.org/10.1029/2001GC000212> (2002).
- Jaffey, A. H., Flynn, K. F., Glendenin, L. E., Bentley, W. C. & Essling, A. M. Precision measurement of half-lives and specific activities of ²³⁵U and ²³⁸U. *Phys. Rev.* **4**, 1889–1906 (1971).
- Ludwig, K. R. *ISOPLOT for MS-DOS, A Plotting and Regression Program for Radiogenic-Isotope Data, for IBM-PC Compatible Computers* version 2.75, Open-File Report 91-445 (US Geological Survey, 1991).
- Ludwig, K. R. *Isoplot 3.70. A Geochronological Toolkit for Microsoft Excel* Vol. 4 (Berkeley Geochronology Center Special Publication, 2003).
- Nilsson, M. K. M. *et al.* Precise U–Pb baddeleyite ages of mafic dykes and intrusions in southern West Greenland and implications for a possible reconstruction with the Superior craton. *Precamb. Res.* **183**, 399–415 (2010).
- Krogh, T. E. A low contamination method for hydrothermal decomposition of zircon and extraction of U and Pb for isotopic age determinations. *Geochim. Cosmochim. Acta* **37**, 485–494 (1973).
- Roddick, J. C. High precision intercalibration of ⁴⁰Ar–³⁹Ar standards. *Geochim. Cosmochim. Acta* **47**, 887–898 (1983).
- Turner, G., Huneke, J. C., Podosek, F. A. & Wasserburg, G. J. ⁴⁰Ar–³⁹Ar ages and cosmic ray exposure ages of Apollo 14 samples. *Earth Planet. Sci. Lett.* **12**, 19–35 (1971).
- Steiger, R. H. & Jäger, E. Subcommission on geochronology: Convention on the use of decay constants in geo- and cosmochronology. *Earth Planet. Sci. Lett.* **36**, 359–362 (1977).